IEEE Access
Multidisciplinary | Rapid Review | Open Access Journal

Received February 17, 2019, accepted February 25, 2019, date of publication March 13, 2019, date of current version March 26, 2019.

Digital Object Identifier 10.1109/ACCESS.2019.2902579

An Efficient Edge Detection Approach to Provide Better Edge Connectivity for Image Analysis

MAMTA MITTAL[1], (Member, IEEE), AMIT VERMA[2], (Life Member, IEEE), IQBALDEEP KAUR[2], BHAVNEET KAUR[3], MEENAKSHI SHARMA[3], LALIT MOHAN GOYAL[4], SUDIPTA ROY[5], AND TAI-HOON KIM[6]

[1]Department of Computer Science and Engineering, G.B. Pant Government Engineering College, New Delhi 110020, India
[2]Department of Computer Science and Engineering, Chandigarh Group of Colleges, Mohali 140307, India
[3]University Institute of Computing, Chandigarh University, Mohali 140413, India
[4]Department of Computer Engineering, J.C. Bose University of Science and Technology, YMCA, Faridabad 121006, India
[5]RCIL, Washington University in Saint Louis, Saint Louis, MO 63110, USA
[6]Department of Convergence Security, Sungshin Women's University, Seoul 136-742, South Korea

Corresponding authors: Sudipta Roy (sudiptaroy01@yahoo.com) and Tai-Hoon Kim (taihoonn@daum.net)

ABSTRACT An edge detection is important for its reliability and security which delivers a better understanding of object recognition in the applications of computer vision, such as pedestrian detection, face detection, and video surveillance. This paper introduced two fundamental limitations encountered in edge detection: edge connectivity and edge thickness, those have been used by various developments in the state-of-the-art. An optimal selection of the threshold for effectual edge detection has constantly been a key challenge in computer vision. Therefore, a robust edge detection algorithm using multiple threshold approaches (B-Edge) is proposed to cover both the limitations. The majorly used canny edge operator focuses on two thresholds selections and still witnesses a few gaps for optimal results. To handle the loopholes of the canny edge operator, our method selects the simulated triple thresholds that target to the prime issues of the edge detection: image contrast, effective edge pixels selection, errors handling, and similarity to the ground truth. The qualitative and quantitative experimental evaluations demonstrate that our edge detection method outperforms competing algorithms for mentioned issues. The proposed approach endeavors an improvement for both grayscale and colored images.

INDEX TERMS Edge, edge connectivity, edge detection, edge width uniformity, threshold.

I. INTRODUCTION

EDGES are directly coupled with shape variations in the distribution of pixel intensities. They carry significant substantiation about an object [1]. Thus, edge detection persistently considered as an elementary operation achieved at low-level image processing and various computer vision applications. The two primary approaches to edge detection from an image are: the thresholding/enhancement technique and the edge fitting technique. The former, depicts the discontinuity in image attributes those are enhanced by processing using operators. The latter, involves in the fitting of / ideal edge pixels. Fig. 1 [2] illustrates the edge enhancement/ thresholding edge detection method. Numerous researchers have committed efforts in designing effective edge operators and its evaluations. In 1981, Kitchen and Rosenfeld [3] made an attempt for detecting the edges based on its local good form by means of a quality evaluation method. The acquired outcomes were similar to consequences obtained from known ideal positions when were compared with the variation in thresholds, noise and blurriness. Non-requirement of the prior information about true locations, made the proposed method applied in multiple applications. Lack in width uniformity was the key limitation of the proposed approach [3]. The work over uniformity, accuracy and sensitivity assessment of edged images was made by Zhu [4]. The improvement in which was made in [5], by working over the partial derivate fails using local information around edge terminals for effective edge linking.

In 1998, Russo [6], adopted the fuzzy reasoning for successful detection of edges without being misled by the noises. Fast and effective outcomes were observed from the

The associate editor coordinating the review of this manuscript and approving it for publication was Mohammad Shorif Uddin.

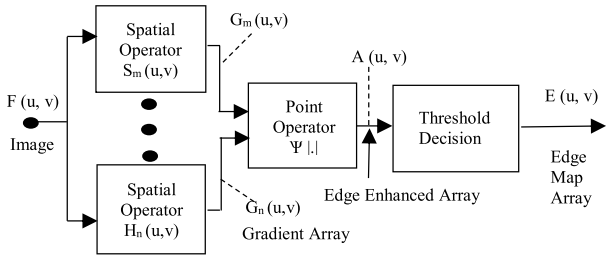

FIGURE 1. Edge enhancement/thresholding edge detection system.

simulations. By the time, an improvement was made in [7] and [8] by using soft-threshold wavelet technique for the removal of noise and practice of Sobel edge detection operator for detection from the image.

Khamy *et al.* [9] took a step towards the improvement of clear edges with an attempt in an improvement of Sobel approach. Lack in satisfactory outcomes led a further enhancement in state-of-the-art using ACO approach [10]. In the year 2006, Dollar *et al.* [11] proposed a supervised learning-based algorithm for edge and boundary detection. In this adaptive learning stage, the algorithm used an extended version of the Probabilistic Boosting Tree classification method for discriminative model learning that selects and amalgamate a huge count of features across various scales.

In the year 2011, Pablo *et al.* [12] target to minimize the image segmentation issues to that of contour detection. He adopted spectral clustering-based globalization contour detection collaborated to multiple detections of local cues. Secondly, he developed a segmentation algorithm with an aim to transform contour detected outcomes into a hierarchical region tree using generic machinery. In the year 2013, Lim *et al.* [13] described a new mid-level feature called sketch tokens that is supervised information in the form of hand drawn contours in images. He clustered the human generated contours patches to generate sketch token classes and random forest classifier for object detection from images.

Agarwal [14] compared the edge detection of bacterial foraging algorithm (BFA) and canny method. It was concluded that BFA obtained better outcomes than canny as bacterial foraging uses swarm intelligence whereas, canny uses gaussian filter. Later, Yang *et al.* [15] aim at the issue of driving relationship between local phase vector and local attenuation, if a higher dimensional signal is not intrinsically one-dimensional signal. To overcome the discussed issue modified differential phase congruency method was developed, which proved a higher dimensional space frequency in it is equal to the minus of the scale derivate of the local attenuation. In the year 2017, Xuan and Hong [16] focus to resolve the limitations of a traditional canny method by introducing differential operation on amplitude gradient histogram. The experiments show that the proposed method was robust to noise and could detach the targets from its background. Later, Verma and Parihar [17], developed a fuzzy system for edge detection by the smallest unvalued segment assimilating nucleus (SUSAN) principal and BFA. Conceptually, a parametric fuzzy intensifier operator (FINT) was developed to improved weak edge information that produces another fuzzy set. BFA was utilized to optimize the involved parameters in fuzzy membership function and FINT. The experiments concluded with acceptable outcomes. Günen and Atasever [18] proposed a backtracking search clustering based edge detection algorithm for noisy images. It was concluded that obtained outcomes performed better than traditional methods even though statistical outcomes vary according to the modified ground truth images. Ma *et al.* [19] proposed a novel de-noising principle based edge detection method on Synthetic Aperture Radar (SAR) images. Outcomes from experiments were obtained to be successful in developing edge visual effect of SAR images and together got down the false edges.

Zhang *et al.* [20] focus to improve the Sobel Edge algorithm by enhancing the gradient template using the FPGA technology. Better outcomes were observed from the improved algorithm. Cao *et al.* [21] work over parallel designed and implementation for an Otsu- optimized canny operator using a Map Reduce parallel programming model. Ostu method aims to optimize the canny operator's dual threshold and performance whereas MapReduce parallel programming operates to resolve speed and cost issues. The outcomes acquired better performance in comparison to the existing methods.

Based on the literature survey, it is observed that the research on edge detection have run parallel and are intermittent from the last 40 years. Incremental progress is reported in successive works for years. Along with this, works are reported from various universities across continents. From the literature review it has been identified that the existing methods lack in accurate detection of edges, fails in edge connectivity and acquiring of optimal qualitative and quantitative analysis. Therefore, in this paper, an effective edge detection algorithm is proposed which successfully comply with the following conditions: 1) The algorithm should have better edge connectivity. 2) The algorithm should provide with improved edge width uniformity. 3) The algorithm must produce acceptable entropy value. 4) The results should have maximum similarity and minimum error to the respective ground truth.

II. PROBLEM CONSTRAIN

Edge detection techniques are classified into two domains: Spatial Domain and Frequency Domain. Basically, spatial domain executes direct operations over the image pixels, such as operator-based methods. Operator based approaches are categorized into first order and second order methods. Technically, first order method estimates the first derivation of image gradient and second order method approximate second derivation of the image gradient. Sobel, Prewitt and Roberts edge detectors are categorized as first order methods and Laplacian & Canny as second order methods, respec-

TABLE 1. Limitations of spatial domain methods.

Operator	Technique	Pros				Cons			
Sobel	SPO1	Simplicity	DEO	NN	NN	SN	Inaccurate	NN	NN
Laplacian	SPO2 /ZC	DEO	FCD	NN	NN	RFEE	SN	NN	LAPLACIAN
Canny	GAUSSIAN	PERROR	LR	ISNR	BDSNC	Complex	Computations	FCD	TC

SPO1- Spatial First Order, SPO 2 -Spatial Second Order, ZC -Zero Crossing, DEO -Detection of edges and their orientation, SN - Sensitivity to noise, FCD -Fixed characteristics in all directions, RFEE -Respond to few existing edges, PERROR -Use probability for error rate finding, LR -Localization and response, ISNR - Improved signal to noise ratio, BDSNC -Better detection specially in noisy conditions, FZC -False zero crossing, TC -Time consumption.

tively. Limitations of Spatial Domain Methods are discussed in Table 1.

Unlike Spatial, an image can be converted into a Frequency Domain using Fourier Transform method. Later to which various operations were performed. Thus, fine details were extracted from low frequencies and corresponding image contour were obtained from high frequencies. Frequency domain carries a limitation of huge search space.

The foremost objective was the rapid and accurate edges detection of object from an image. In the initial phase, an attempt for effective edge detection was made by Gonzalez and Woods [22]. Prewitt operator was a discrete differentiable operator that computes the gradient of an image intensity function. It was limited to eight possible orientations, from which the majority were not accurate. Though it was easy to implement yet it was highly sensitive to noise.

Later, first order differential-based edge detection approach was developed, named Sobel edge detection algorithm. The gradient was a ration of a functional variation and an image can be considered as a sampling point group of continuous functions of a gray image. Therefore, substantial variations in the value of a gray image can be verified using discrete approach gradient functions. The major issue with the Roberts operator was its sensitivity to noise while evaluation of direction difference. Thus, Sobel proposed an omnidirectional differential operator, having a partial derivative in m and n direction. It was a3 × 3 convolution kernelled row edge operator [9] of point $E(c, d)$, namely

$$\left.\begin{aligned} A_c &= \{E(c+1, d-1)+(2 \times E(c+1, d))+E(c+1, d+1) \\ &\quad -\{E(c-1, d-1)+(2 \times E(c-1, d)) \\ &\quad +E(c-1, d+1) \\ A_d &= \{E(c-1, d+1)+(2 \times E(c, d+1))+E(c+1, d+1) \\ &\quad -\{E(c-1, d-1)+(2 \times E(c, d-1)) \\ &\quad +E(c+1, d-1) \end{aligned}\right\} \tag{1}$$

The above formula applies weightage average difference of image intensity in neighborhood of $E(c, d)$. Here, the gradient directs at the highest variation of the function $E(c, d)$ and its size can be computed from (2)

$$G(c, d) = \sqrt{A_c^2 + A_d^2} \tag{2}$$

Equation (2) presents that the gradient amplitude $E(c, d)$ was intensified unit distance in the direction of the highest rate change. For digital images the mentioned (2) is further reduced to (3).

$$G(c, d) = |A_c| + |A_d| \tag{3}$$

Sobel was a weighting algorithm which detects the edge by weighting all the adjacent point pixels in each direction (Left, Right, Up and Down) and identifies edge according to phenomena that it can reach to extreme value in the edge points.

Thus, Sobel obtains smooth effect over noise but the magnitude of the edges degrades drastically which leads to the production of false edges and extreme low pixel localization due to the influence of local average concept. Therefore, Sobel was not preferred edge detection approach for high accuracy.

By 1986, a widely known Canny operator was proposed by Canny [23]. The canny operator uses a Gaussian filter to

TABLE 2. Classification of physical measures of edge quality and their quality indices.

Edge Quality	Explanation	Remarks
Continuity	$C = (1 + bN_c)^{-1}$	C Continuity Index b Break counts in detected edge N_c Normalization Constant
Thinness	$T = A_w$	T Thinness Index A_w Average Width
Smoothness	$S = (1 + E_r)^{-1}$	S Smoothness Index E_r Edge Roughness
Detection	$D = d$	D Detection Index d Truth Edge Detection Percentage
Localization	$L = (1 + L_e)^{-1}$	L Localization Index L_e Location Error Average (displacement from center)
Noisiness	$N = \begin{cases} 1.\ (1 + mC_m)^{-1} - 1 \\ 2.\ (1 + m`C_{m`})^{-1} - 1 \end{cases}$ When distance between noisy pixel and edges in not essential; Option 2 is made under consideration. Else option 1	N Noisiness Index m Σ (1 / all distances from noisy pixels to true edge) m` Noisy pixels count $C_m$ Normalization Constant $C_{m`}$ Normalization Constant
Edge Quality Score	$EQ\_S = w_cC + w_sS + w_TT + w_LL + w_dD + W_mN$	w_c depicts the weighting factor of C, w_s depicts weighting factor of S, etc.

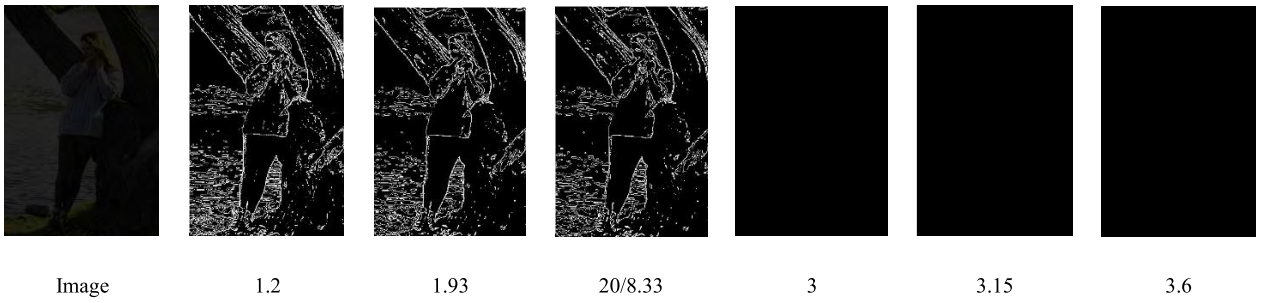

FIGURE 2. Edge detection can be easily performed on normal images but there is always an issue in the processing with low contrast images. Therefore, simulations are performed on such images with an aim to identify an intensity, for generating the final image fit for edge detection. It has been identified that intensity below 20/8.33 causes double edges and automatic noise generation. Whereas, intensity above 20/8.33 causes highly smooth image with no edge information.

smooth the image and for noise removal.

$$d = \frac{\{8 \times (\phi) - 1\}}{2} \tag{4}$$

Once the gradient magnitude has been computed non-maximum suppression was applied, where the algorithm eliminated the non-edge pixels.

$$Guass\ Kernal = \frac{1}{\sqrt{2\pi} \times \phi}.exp\left[\frac{-\left(E^2\right)}{2 \times (\phi)^2}\right] \tag{5}$$

Basically, smoothing of an image was performed using Gaussian filter and reduction in noise was made specific of particular standard deviation σ. Computation of the gradient magnitude for partial derivatives using finite-difference approximations over which non-Maxima suppression was applied.

If $I[u, v]$ was an image. Gaussian Smoothing Filter was presented as $G_s[u, v, \delta]$, where δ depicts the Gaussian spread and manage the smoothness degree.

$$S_m[u, v] = G_s[u, v, \delta] \cdot I[u, v] \tag{6}$$

$S_m[u, v]$ was smoothed array used to compute α and β partial derivatives *A [u, v] and B [u, v]* as:

$$\begin{aligned} A[u, v] \approx\ & (S_m[u, v + 1] - S_m[u, v] \\ & + S_m[u + 1, v + 1] - S_m[u + 1, v])\ /2 \\ B[u, v] \approx\ & (S_m[u, v] - S_m[u + 1, v] \\ & + S_m[u, v + 1] - S_m[u + 1, v + 1])\ /2 \end{aligned}$$

By averaging finite differences, the computation of α and β partial derivatives were made. Gradient magnitude and orientation were figured as:

$$M_g\,[u, v] = \sqrt{A[u, v]^2 + B[u, v]^2} \tag{7}$$

Finally, hysteresis thresholding was applied along the edges. Basically, hysteresis used two thresholds: upper threshold and lower threshold. Here, the pixel gradient above the upper threshold was marked as an edge and the pixel gradient below the lower threshold was discarded. If the pixel gradient lies between the two thresholds, it would be considered as candidate edge points. The candidate edge points in connection with edge edges would be considered as an edge.

Technically, canny use non-maxima suppression method for enhancing the signal w. r. t. noise ratio, as the suppression method results in one-pixel wide ranges as the outcome. The canny edge detector has few of loopholes such as: 1) It lacks in time consumption. 2) The use of the huge count of parameters in the canny edge operator algorithm leads to infinite tweaking for obtaining a little better result. 3) There is still a need of connecting the resulting edges for extraction of complete edges those are obvious from the human perspective. 4) The Gaussian smoothing causes a lack in the localization of the detected edges (it directly depends on the size of Gaussian kernel). 5) Gaussian smoothing causes a blurriness in the corners, junctions and edges. 6) The corner pixels lead in open-ended edges and missing junctions.

In later year, Rong *et al.* [24] proposed an improved Canny Edge Detection Algorithm (ICA). Firstly, a gravitational field intensity concept had been introduced in the algorithm to replace the image gradient that was earlier used in traditional canny edge operator. Secondly, developed two adaptive threshold selection methods for an image with less and rich edge information. In ICA the templates of the image gradient with a2 $\times$ 2 neighboring area operator are improved with a replacement to 3 $\times$ 3 neighboring area operator.

Traditional Canny Edge operator had 2 $\times$ 2 neighboring area operator as: $G_x = \begin{bmatrix} -1 & 1 \\ -1 & 1 \end{bmatrix}$ and $G_y = \begin{bmatrix} 1 & 1 \\ -1 & -1 \end{bmatrix}$. And the ICA has improved to 3 $\times$ 3 neighboring area operator as:

$$G_x = \begin{bmatrix} -\frac{\sqrt{2}}{4} & 0 & \frac{\sqrt{2}}{4} \\ -1 & 0 & -1 \\ -\frac{\sqrt{2}}{4} & 0 & \frac{\sqrt{2}}{4} \end{bmatrix}$$

and

$$G_y = \begin{bmatrix} \frac{\sqrt{2}}{4} & 1 & \frac{\sqrt{2}}{4} \\ 0 & 0 & 0 \\ -\frac{\sqrt{2}}{4} & -1 & -\frac{\sqrt{2}}{4} \end{bmatrix}.$$

The edges in image only occupy a little part, therefore an inversely proportional relation had been observed between gradient magnitude of the edge pixels ad edge pixels count.

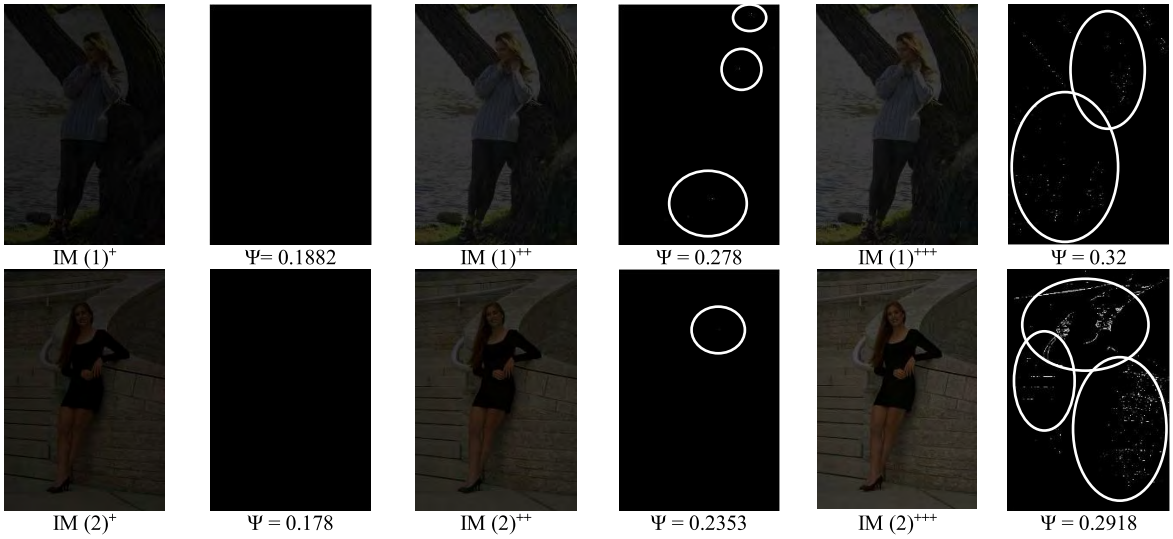

FIGURE 3. Performing edge detection on low contrast image has always been a challenging chore in computer vision. Therefore, the proposed algorithm step forward to minimize the low performance rate on such images. Firstly, to verify the suitability of the inputted image for edge detection gray thresh value is calculated by the proposed algorithm. It has been witnessed that computed gray thresh value sometimes falls in a situation when image turns unfit for result generation because of a lack in image contrast. Therefore, conduct of simulative experiment is made to identify the minimum threshold value below which image turns unfit. From the experiment it has been analyzed that threshold value below 0.2 fails in acquiring of edges from an image (As presented in IM $(1)^{+}$ and IM $(2)^{+}$). Whereas on increasing the contrast of an image to an extent (As presented in IM $(1)^{++}$, IM $(1)^{+++}$, IM $(2)^{++}$ and IM $(2)^{+++}$), proposed algorithm results to a threshold value 0.2 and above, respectively. It has successfully led to a generation of edges from the corresponding images (the slightly generated edge pixels are encircled). Lastly, with an aim to increase the contrast of an image, imadjust() is called. Finally, the complete process is executed again on the adjusted image. (Detailed discussion in made in Step-3 of Section-3).

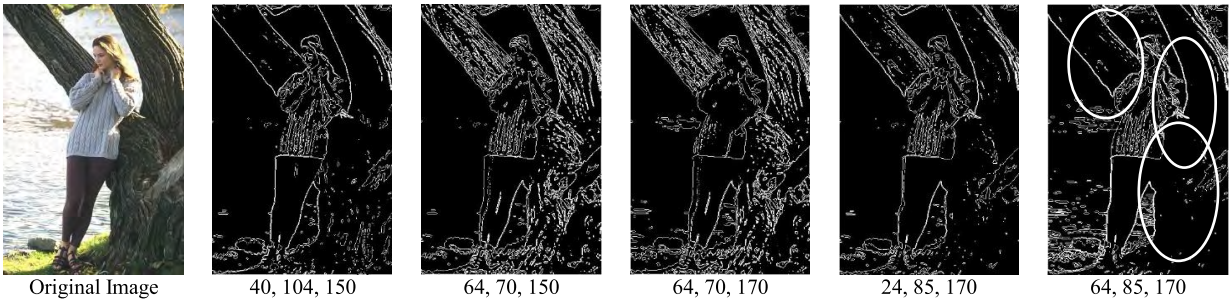

FIGURE 4. The proposed method handled the other limitation of edge detection i.e. Edge Connectivity with an implementation of triple intensity thresholds. Simulations are performed on an image with an aim to achieve a complete coverage to the grayscale intensity range such that no intensity lead to generation of compromising edge detection outcomes. Multiple combinations were selected for simulations (as presented in above images) but the combination of 64, 85 and 170 not only provided the complete coverage to the grayscale intensity range but also lead to a generation of more connected edges with an improved noise handling in the image.

Hence, selection of threshold had a great relationship with the mean of gradient magnitude and standard deviation. For images with less edge information the gradient magnitude of majority of the pixels was located in a small range in images, which ends up to a relatively small mean of gradient magnitude and the standard deviation. Thus double-threshold selection method for such images had been made under consideration. Whereas, in images with a large field of view, the contrast of each part of the entire image was inconsistent, and the image gradient's standard deviation was large relatively. Therefore, for this kind of images, a selection to double-threshold for each pixel was made under consideration. Finally, it had been identified even the ICA not only keeps the advantages of the traditional Canny algorithm, but also it enhances the ability of noise suppression and edge information. But its computing speed was relatively slow and when analyzed qualitatively, a further improvement is still required.

Thus, to overcome the drawbacks of the above studied approaches, a new efficient edge detection algorithm is proposed. The major edge quality measures which should always be considered for effective outcomes in the state-of-the-art are discussed in Table 2.

III. PROPOSED ALGORITHM

This section covers a detailed discussion of the proposed algorithm (B-Edge). The pictorial flow of the data in the algorithm is presented in Fig. 5. The algorithm is as follows:

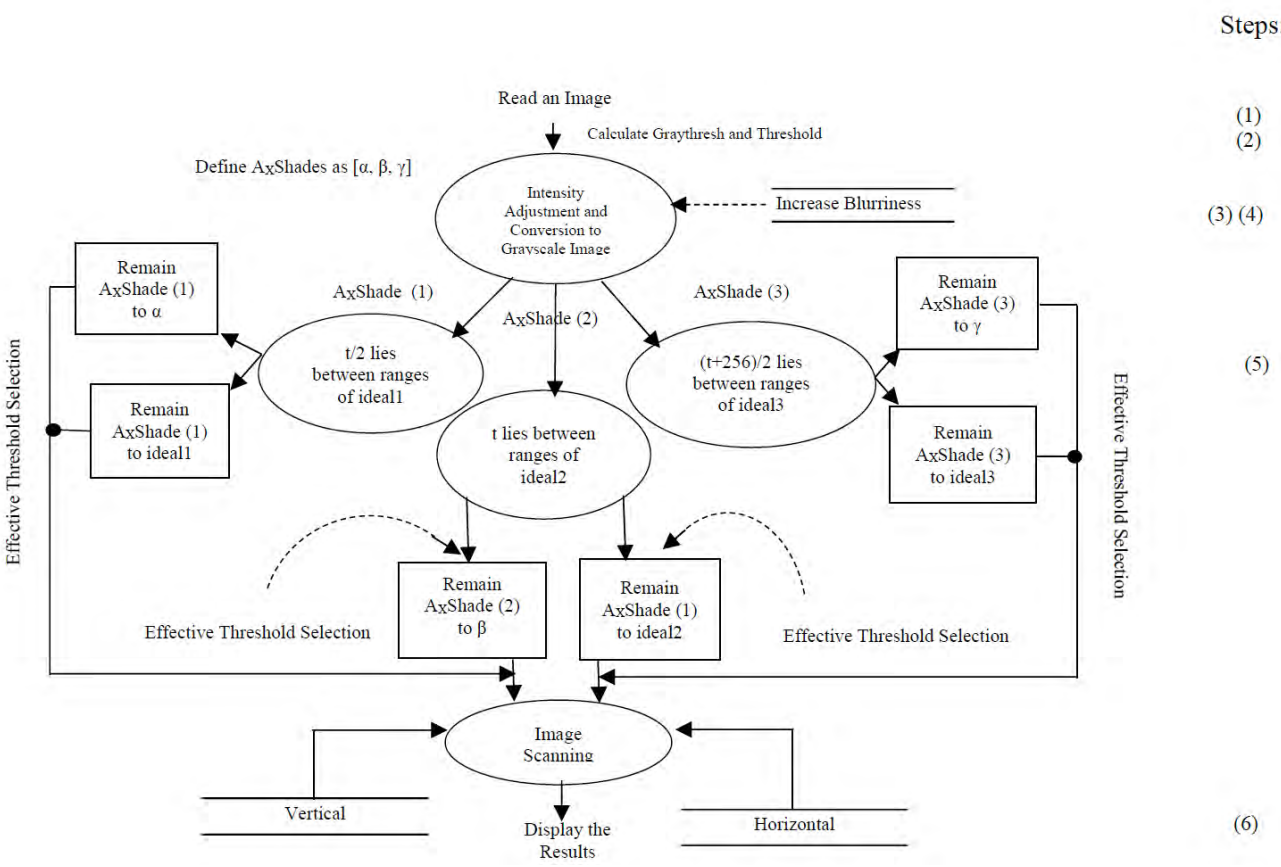

FIGURE 5. Data flow diagram of the proposed algorithm.

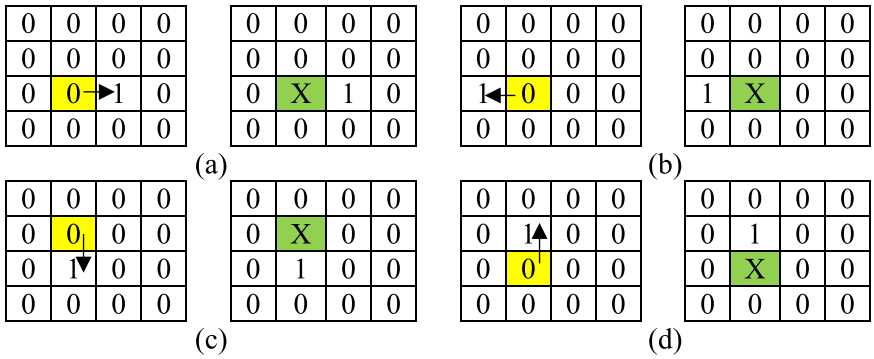

FIGURE 6. Process over the pixels for edge formation in all the four directions: (a) the current pixel is considered to be an edge pixel, if the value of right pixel is larger than the selected threshold. (b) If the value of left pixel is larger than the selected threshold, the current pixel is considered to be an edge pixel. (c) If the value of below pixel is larger than the selected threshold, the current pixel is considered to be an edge pixel. (d) The current pixel is considered to be an edge pixel, only if the value of above pixel is larger than the selected threshold.

Step-1: The image I_{img}, is read from the database.

Step-2 (Graythresh and Threshold Computation Phase): The graythresh of each pixel is computed by (8),

$$\psi = \frac{\left(\sum_{\alpha=1}^{n} \sum_{\beta=1}^{m} ara\right)}{m \cdot n} \tag{8}$$

Here, m and n depict the pixel dimensions and ara is an array of an input image. Graythresh provides an average of an image, which is different for every inputted image.

Step-3 (Intensity Adjustment Phase): The corresponding threshold value (ϕ) of an image is then computed by (9),

$$Phi = \frac{\psi \cdot 20}{8.33} \tag{9}$$

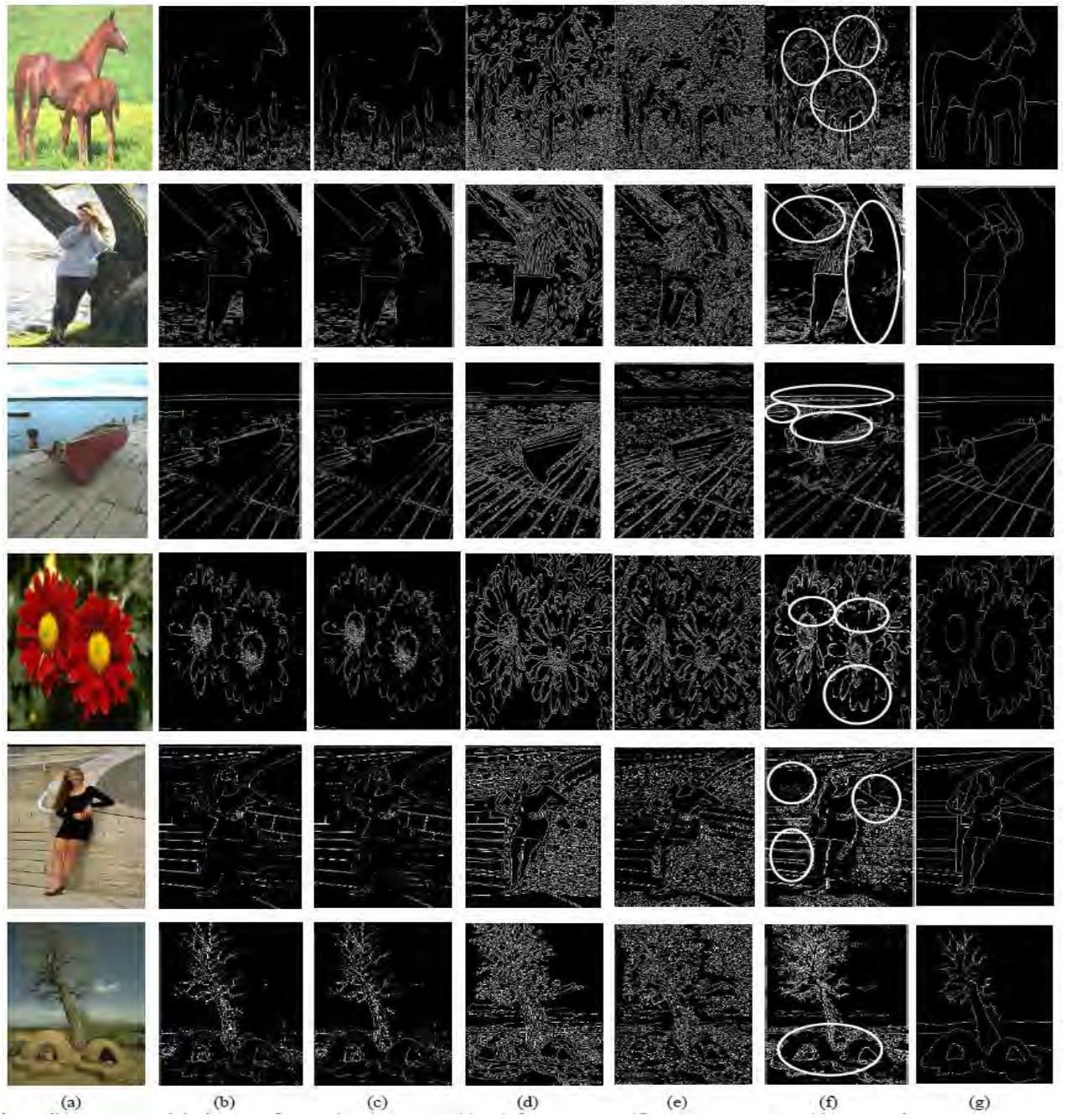

FIGURE 7. Illustrates (a) original Image. (b) Prewitt's Outcomes. (c) Sobel's Outcomes. (d) Canny's Outcomes. (e) Improved Canny's Outcomes. (f) Our Outcomes. (g) Ground Truth.

With an aim to increase the contrast of an image I_{img}, the computed Ψ is multiplied with a constant 20/8.33. The constant 20/8.33 is made under consideration because as per the further simulative experiment it has been witnessed that a value greater than 20/8.33, results to a higher Φ value. This leads to an implementation of the additional step of blurriness with a high magnitude which results in high smoothness in an image that causes a reduction in edge information. Whereas, a lesser value than 20/8.33, results to a lower Φ value. This leads to an implementation of blurriness with a low magnitude which results in double edges and automatic noise generation which minimized the generation of acceptable outcomes (See Fig. 2). Here, the computed value of Φ sometimes falls in a situation when image I_{img} turns unfit to obtain a result because of the lack in image contrast. Therefore, a conduct of simulative experiment is made to identify the minimum Φ value below which I_{img} turns unfit. From the simulative experiments it has been identified that the intensity of an

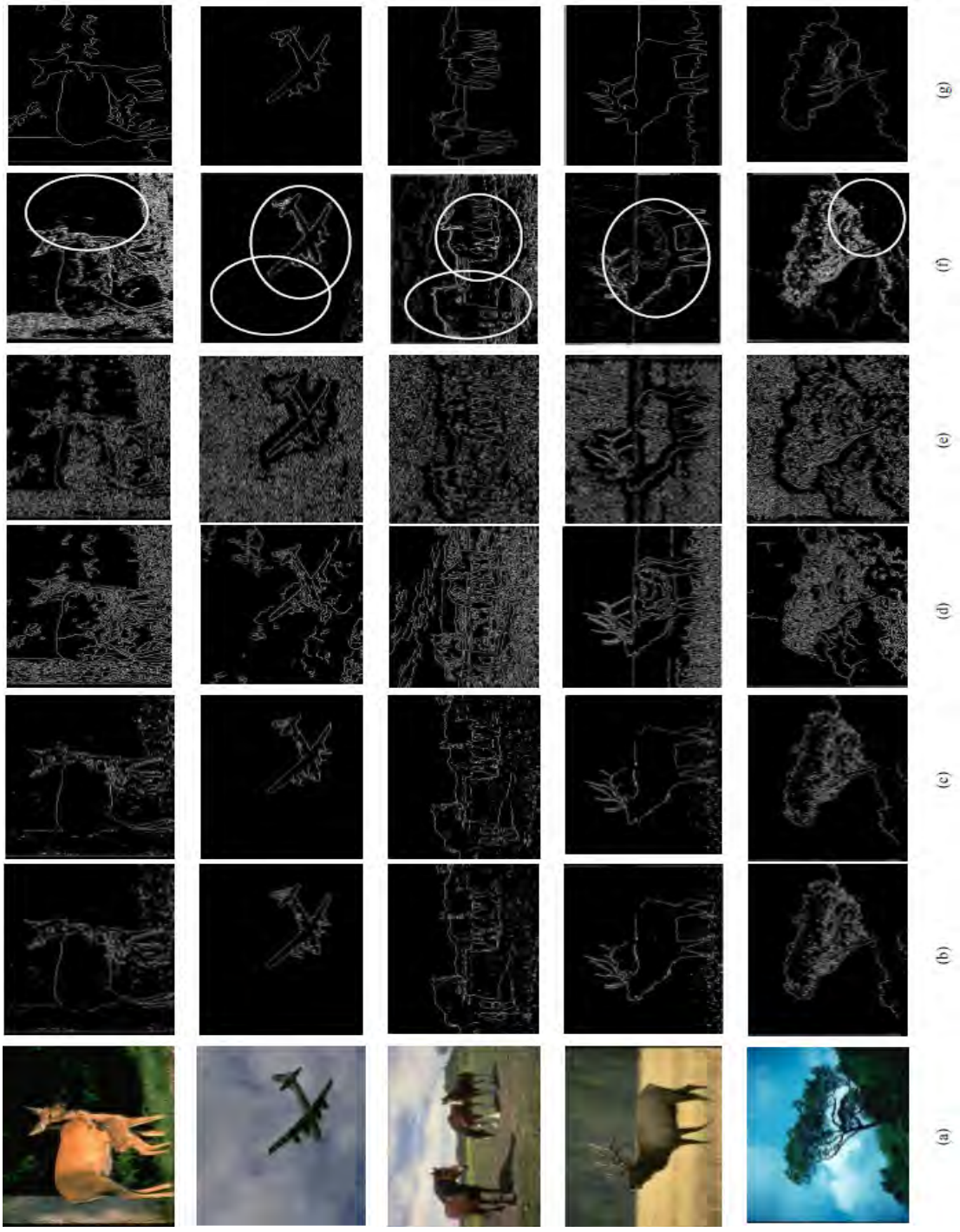

FIGURE 8. Illustrates (a) original Image. (b) Prewitt's Outcomes. (c) Sobel's Outcomes. (d) Canny's Outcomes. (e) Improved Canny's Outcomes. (f) Our Outcomes. (g) Ground Truth.

image below 0.2 results in a black outcome due to low contrast and unsatisfactory presence of the color difference in the image. Thus, our target is to increase the image contrast (See Fig. 3). ''imadjust()'' function is called in the proposed method with an aim to automatically increase the image contrast. Thus, with an implementation of the blurriness effect in an algorithm our method handles the first limitation of edge detection i.e. ''Edge Thickness'' satisfactorily.

Step-4 (Grayscale Conversion Phase): A grayscale image technically variates in an intensity range of 0-255. From the literature review it has been identified that an optimal selection of the threshold for effectual edge detection has constantly been a key challenge in computer vision. It has been noted that a non-consideration to complete intensity range has always resulted to insufficient improvement in edge detection. Even double threshold method of Canny edge

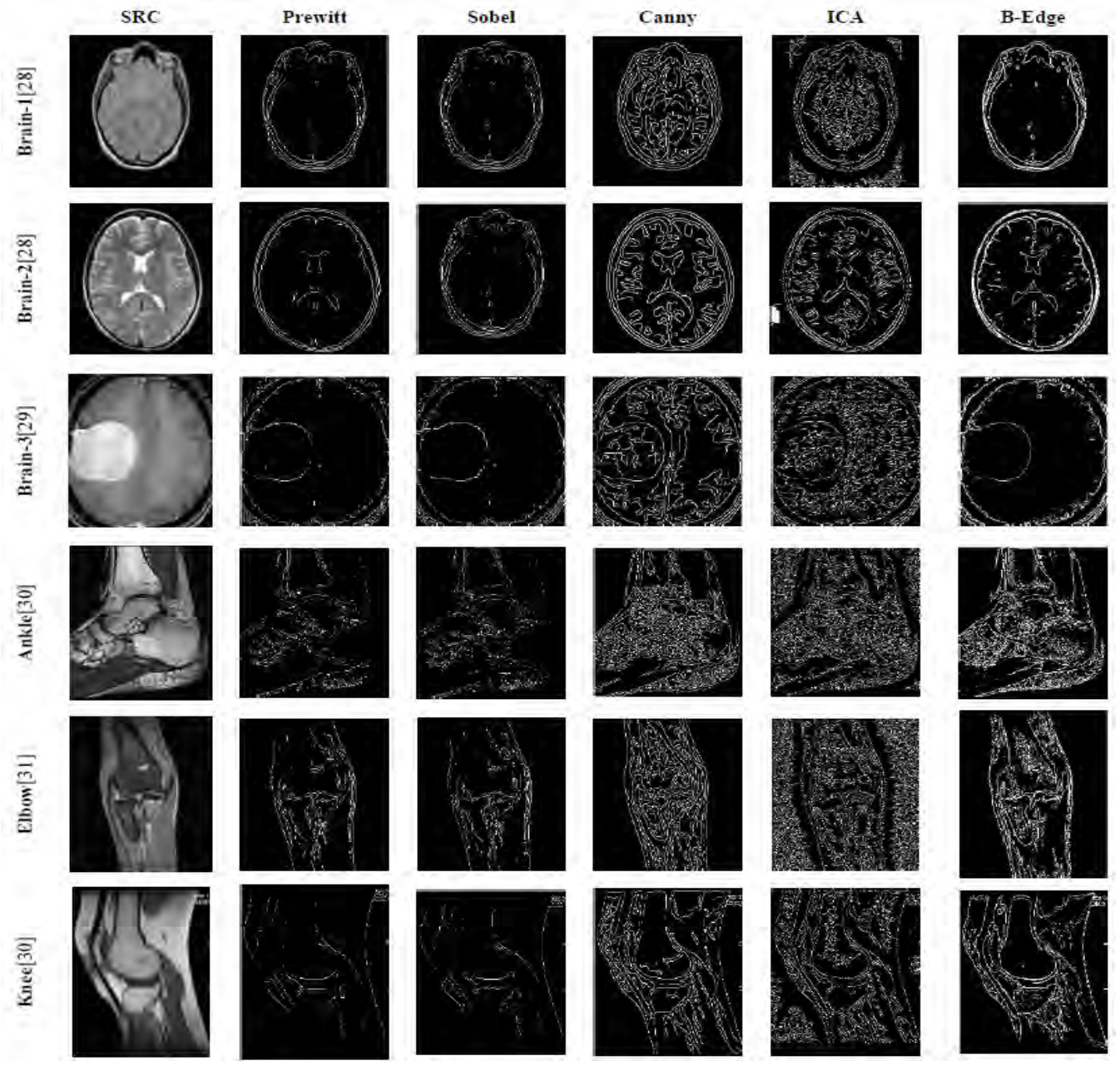

FIGURE 9. The results in comparison of previously proposed methods through entropy on various human body parts.

operator detects the edge rely on gradient magnitude-based information, which requires an improvement in edge connectivity and image information. Therefore, a multiple threshold approach is used in our proposed method.

Here, triple intensity threshold values set as α, β, γ have been defined that aims a complete coverage to the grayscale intensity range such that no intensity leads to a generation of compromising edge detection outcome. In this method, the threshold selection is based on automatic simulated results conducted in color processing. From the simulations 64, 85 and 170 are selected as best possible intensity values for contributing an improvement in edge detection (See Fig. 4). To ensure acceptable outcomes the image I_{img} is firstly converted to grayscale by (10).

$$ara\,(\alpha, \beta) = \frac{\sum (ara\,(\alpha, \beta, :))}{3} \tag{10}$$

where, $\alpha \in \{1, 2, \cdots, n\}$ and $\beta \in \{1, 2, \cdots, n\}$. Here, intensities 64, 85 and 170 are made under consideration because it is witnessed that the intensity 64 fulfills the requirement of low intensities for appropriate edge detection and its property also matches to properties of intensities greater than 220. Whereas, intensity 85 majorly carries a grayscale shade that falls between the range 70-120 and its property also matches

TABLE 3. Parametric evaluation of selected images through entropy difference.

Images	Prewitt	Sobel	Canny	ICA	B-Edge
IM-1	0.1548	0.1573	0.4835	0.5247	**0.3873**
IM-2	0.1208	0.1203	0.4662	0.4914	**0.2430**
IM-3	0.1096	0.1079	0.3031	0.3758	**0.1794**
IM-4	0.1674	0.1672	0.2796	0.4035	**0.2579**
IM-5	0.0741	0.0746	0.2139	0.5347	**0.0929**
IM-6	0.1177	0.1172	0.2260	0.4699	**0.2162**
IM-7	0.1895	0.1871	0.4410	0.3920	**0.4123**
IM-8	0.1190	0.1197	0.2230	0.4189	**0.1848**
IM-9	0.1465	0.1472	0.3300	0.1416	**0.2898**
IM-10	0.0449	0.0444	0.2666	0.4562	**0.0861**
IM-11	0.1136	0.1158	0.2758	0.3599	**0.1535**
IM-12	0.1802	0.1845	0.4282	0.4621	**0.3626**
IM-13	0.1186	0.1193	0.2705	0.4778	**0.2131**
IM-14	0.1141	0.1164	0.4130	0.6378	**0.1734**
IM-15	0.0891	0.0912	0.2088	0.4738	**0.0827**
IM-16	0.1193	0.1214	0.3102	0.3908	**0.1522**
IM-17	0.0747	0.0751	0.1937	0.4199	**0.1000**
IM-18	0.1630	0.1640	0.3170	0.3826	**0.2676**
IM-19	0.1950	0.1953	0.6461	0.6071	**0.2562**
IM-20	0.1299	0.1298	0.2738	0.3148	**0.2025**
IM-21	0.0936	0.0960	0.2683	0.4634	**0.1607**
IM-22	0.0881	0.0900	0.2503	0.3706	**0.1240**
IM-23	0.0969	0.0973	0.2853	0.4911	**0.1878**
IM-24	0.1928	0.1945	0.3575	0.4586	**0.3202**
IM-25	0.0634	0.0639	0.3664	0.4216	**0.0952**
IM-26	0.1751	0.1762	0.4602	0.5080	**0.1908**
IM-27	0.1843	0.1850	0.4695	0.4691	**0.3157**
IM-28	0.0945	0.0962	0.3581	0.4064	**0.0993**
IM-29	0.1608	0.1622	0.3356	0.5548	**0.1083**
IM-30	0.1371	0.1386	0.3680	0.4846	**0.1403**

to properties of intensities closer to 135. In the case of intensity 170, if the intensity value slightly changes, then it leads to the creation of double edges. Thus, selecting these triple intensities delivers a complete coverage to intensity range, therefore leads to effective edge detection with improved edge connectivity. This algorithm can obtain threshold automatically, which has higher practical value in the practical engineering application.

Step-5 (Best Solution Selection): An appropriate range check has been examined. The individual threshold that falls under ideal range of shortlisted intensities is considered as one of the three finalized thresholds for the edge detection than the latest obtained. Unlike to the above scenario, if the individual threshold would not fall under ideal range, then the general threshold is continuing to take its respective position for the threshold. Initialize a zero array O to any user defined size $[\alpha, \beta]$. Once the three thresholds are identified from above operations than the scanning over the pixels in the horizontal direction is applied and detected edge pixels of the object will be updated in the empty array O (as described in Fig. 6). Finally, the array is called and the resultant edged image is revealed. It is performed as,

if (ara $(\alpha - k, \beta - \mathrm{k}) >$ *Selected Thresholds*(Φ))

Update O (α, β) *by 1*

Where, $\alpha \in \{1, 2, \ldots, n\}, \beta \in \{1, 2, \ldots, n\}$ and $k \in \{-1, 0, 1\}$

Step-6: Repeat the step 5 with respect to vertical direction now.

IV. SIMULATION RESULTS WITH PERFORMANCE ANALYSIS

Using the Berkeley dataset (BSDS500) the proposed edge detection algorithm has been evaluated both qualitatively

TABLE 4. Parametric evaluation of selected images through MSE.

Images	Prewitt	Sobel	Canny	ICA	B-Edge
IM-1	0.15597	0.15673	0.17082	0.32940	**0.14685**
IM-2	0.14734	0.14729	0.15686	0.28950	**0.09797**
IM-3	0.15931	0.16111	0.13635	0.31830	**0.09585**
IM-4	0.16223	0.16199	0.11671	0.36080	**0.11524**
IM-5	0.13330	0.13354	0.08525	0.28010	**0.04550**
IM-6	0.13530	0.13503	0.07159	0.13810	**0.07078**
IM-7	0.15850	0.15745	0.14240	0.13470	**0.14175**
IM-8	0.15142	0.15170	0.10331	0.14199	**0.09075**
IM-9	0.16933	0.16949	0.14372	0.14160	**0.13991**
IM-10	0.13170	0.13143	0.08902	0.14100	**0.04619**
IM-11	0.14164	0.14230	0.09997	0.11270	**0.06220 8**
IM-12	0.15579	0.15653	0.15114	0.15200	**0.13701**
IM-13	0.14470	0.14488	0.09821	0.14520	**0.08516**
IM-14	0.13745	0.13782	0.12766	0.19240	**0.06650**
IM-15	0.13226	0.13311	0.07231	0.15140	**0.03703**
IM-16	0.14093	0.14152	0.10654	0.12181	**0.05531**
IM-17	0.13260	0.13262	0.07763	0.13727	**0.03714**
IM-18	0.15371	0.15402	0.10484	0.11311	**0.10098**
IM-19	0.15486	0.15424	0.24302	0.20833	**0.09355**
IM-20	0.15150	0.15168	0.11152	0.11736	**0.08903**
IM-21	0.13160	0.13225	0.08714	0.13462	**0.05459**
IM-22	0.14333	0.14358	0.09447	0.11602	**0.06180**
IM-23	0.14650	0.14631	0.10521	0.16043	**0.08690**
IM-24	0.17968	0.18210	0.17828	0.19799	**0.14607**
IM-25	0.13620	0.13629	0.12181	0.13122	**0.04835**
IM-26	0.14567	0.14574	0.14651	0.14984	**0.05902**
IM-27	0.15342	0.15339	0.15869	0.15590	**0.11985**
IM-28	0.14225	0.14247	0.12469	0.13431	**0.04878**
IM-29	0.15356	0.15391	0.12315	0.17359	**0.04448**
IM-30	0.15043	0.15093	0.12708	0.15352	**0.06144**

and quantitatively. BSDS500 is an extension of BSDS300, encompasses original 300 images for validation/ training 170 and 200 images for testing [12], [13]. This benchmark operates by performing comparisons between machine-generated contours and ground truth data are shown in Fig. 7-9, that allows segmentation assessment in a similar framework by concerning region boundaries as contours.

A. QUALITATIVE ANALYSIS

Qualitative assessment of obtained outcomes together with the outcomes of four major benchmarked edge detection algorithms [9], [22]–[24] are shown in Fig. 7-9. Fig. 7-8 (a) present images selected for operations. Fig. 7-8 (b-e) correspondingly, displays the results of Prewitt [22], Sobel [9] Canny [23] and Improved Canny (ICA) [16]. The outcomes of the proposed algorithm (B-Edge) are displayed in Fig. 7-8 (f). Prewit's and Sobel's results are marginally similar to the ground truth as less continuity in the detected edges are identified but many more enhancements have been observed from the Canny's results, which are much similar to the ground truth images. On observation, over-segmentation has been identified in the results of Sobel. Since Sobel effectively highlights noise initiated in real world pictures, the detected edges are analyzed to be thicker in comparisons to the other (See Fig. 7-9 (c)). Unlike these, the outcomes from Canny's method have more connected edges. Even then, in some cases double edges are encountered by Canny (Fig. Fig. 7-8 (d)). A minute enhancement in the Canny method is observed with the implementation of ICA (See Fig. Fig. 7-8 (e)).

TABLE 5. Parametric evaluation of selected images through PSNR.

Images	Prewitt	Sobel	Canny	ICA	B-Edge
IM-1	**57.6852**	57.6268	55.8394	52.9867	56.4960
IM-2	58.4127	58.4175	56.2097	53.5480	**58.4538**
IM-3	57.4338	57.3034	56.8184	53.1361	**58.3487**
IM-4	57.2245	57.2413	57.4938	52.5920	**57.5488**
IM-5	59.9408	59.9088	58.8578	53.6909	**61.5848**
IM-6	59.6865	59.7201	59.6161	56.7609	**59.7655**
IM-7	57.4935	**57.5716**	56.6604	56.8704	56.6494
IM-8	58.0536	58.0302	58.0234	56.6421	**58.5863**
IM-9	56.7558	56.7457	56.5897	56.6536	**56.7864**
IM-10	60.1547	60.1921	58.6699	56.6649	**61.5198**
IM-11	58.9699	58.9015	58.1662	57.6448	**60.2263**
IM-12	**57.6993**	57.6422	56.3710	56.3277	56.7972
IM-13	58.6622	58.6440	58.2432	56.5443	**58.8627**
IM-14	59.4298	59.3879	57.1044	55.3216	**59.9364**
IM-15	60.0781	59.9654	59.5727	56.3617	**62.4796**
IM-16	59.0441	58.9827	57.8896	57.3081	**60.7367**
IM-17	60.0330	60.0296	59.2646	56.7890	**62.4667**
IM-18	57.8642	57.8396	57.9596	57.6299	**58.1226**
IM-19	57.7725	57.8220	54.3083	54.9773	**58.4544**
IM-20	58.0471	58.0318	57.6912	57.4695	**58.6692**
IM-21	60.1680	60.0790	58.7628	56.8738	**60.7941**
IM-22	58.7970	58.7718	58.4119	57.5196	**60.2549**
IM-23	58.4901	58.5082	57.9441	56.1119	**58.7744**
IM-24	56.1515	56.0211	55.6537	55.1983	**56.5191**
IM-25	59.5780	59.5671	57.3081	56.9849	**61.3204**
IM-26	58.5682	58.5620	56.5060	56.4084	**60.4552**
IM-27	57.8878	**57.8904**	56.1593	56.2364	57.3784
IM-28	58.9068	58.8836	57.2065	56.8836	**61.2828**
IM-29	57.8768	57.8485	57.2606	55.7695	**61.6836**
IM-30	58.1376	58.0954	57.1239	56.3033	**60.2805**

Although the B-Edge did not satisfactorily detect the complete background edges in the Row-1 of the Fig. 7 as presented in the corresponding ground truth but it has successfully identified the object's edges. Even, a discontinuity can be observed from the ICA's outcome for the same image. Maximum identical edges to the corresponding ground truths have been identified by the B-Edge in Row- 6 of Fig. 7, and Row- 4 & 5 of Fig. 8. High edge connectivity has been witnessed in Row- 2 & 5 of Fig. 7 and Row- 2, 3 & 4 of Fig. 8. In case of noise handling, acceptable results have been acquired and observed by the proposed method in Row- 1, 2, 4 & 6 of Fig. 7 and Row- 1, 3, 4 & 5 of Fig. 8. In contrast, high noise occurrence can be noticed from the outcomes of the existing algorithms.

Despite all, the proposed algorithm is efficiently managing over-segmentation issues, edge continuity, uniformity of the detected edges and has preserved more local edge information. Like the above images, the proposed algorithm B-Edge is applied over the MR images of various human body parts such as elbow, ankle, knee and brain. The results are presented in Fig. 9. On the execution of the B-Edge on human body parts it is witnessed that the proposed algorithm obtains the improved outcomes in comparison to the existing methods by efficiently handling noise, double edges, edge connectivity and entropy. In image Brain-3, B-Edge effectively identified the tumor using edges, whereas from the outcomes of Prewitt and Sobel a huge edge disconnection is observed which made these methods inappropriate for analysis of medical images. Unlike to Prewitt and Sobel, ICA turns unable to handle the noise which leads to high entropy values. In case of Brain-1 and Brain-2 double edges and low information content are witnessed from Prewitt and Sobel. Where ICA obtained the edges from background region of an image which leads to high entropy value. In image ankle, knee and elbow high edge discontinuity can be observed from the outcomes of Prewitt & Sobel and high noise presence can be witnessed from the outcomes of ICA for the respective images.

B. QUANTITATIVE ANALYSIS

A complete quantitative assessment through Entropy [25], MSE (Mean Squares Error), PSNR (Peak Signal to Noise Ratio) [26] & finally the SSIM (Structural Similarity Index) [27] is discussed in this section. The outcomes of the quantitative analysis are presented in Fig. 7-9.

TABLE 6. Parametric evaluation of selected images through SSIM.

Images	Prewitt	Sobel	Canny	ICA	B-Edge
IM-1	**0.4053**	0.4020	0.1982	0.0154	0.2273
IM-2	0.4594	0.4565	0.2453	0.0621	**0.5236**
IM-3	0.3915	0.3839	0.3601	0.1283	**0.4796**
IM-4	0.3507	0.3509	0.3576	0.0923	**0.3989**
IM-5	0.5431	0.5392	0.5869	0.0751	**0.6549**
IM-6	0.5236	0.5221	0.5728	0.1662	**0.5837**
IM-7	0.4105	**0.4111**	0.3416	0.1555	0.3345
IM-8	0.4682	0.4651	0.5242	0.1821	**0.5716**
IM-9	0.3520	0.3503	0.3102	0.1432	**0.3637**
IM-10	0.6300	0.6308	0.4323	0.1865	**0.7199**
IM-11	0.4938	0.4885	0.4696	0.2494	**0.6293**
IM-12	0.3236	0.3161	0.2977	0.1868	**0.3466**
IM-13	0.5211	0.5192	0.4955	0.1495	**0.5405**
IM-14	0.5121	0.5048	0.3339	0.0302	**0.6009**
IM-15	0.5691	0.5643	0.5697	0.1219	**0.7536**
IM-16	0.4625	0.4603	0.4242	0.2505	**0.6356**
IM-17	0.5736	0.5697	0.5966	0.2521	**0.7548**
IM-18	0.3915	0.3871	0.4550	0.2545	**0.5242**
IM-19	0.1910	0.1888	0.0974	0.0183	**0.3875**
IM-20	0.4173	0.4168	0.4889	0.3466	**0.4909**
IM-21	0.5454	0.5424	0.5134	0.1799	**0.5697**
IM-22	0.5228	0.5197	0.4773	0.2277	**0.6270**
IM-23	0.5213	0.5178	0.4841	0.1447	**0.5878**
IM-24	0.2795	0.2746	0.3064	0.0968	**0.3374**
IM-25	0.5828	0.5783	0.3367	0.1926	**0.6960**
IM-26	0.3621	0.3586	0.2781	0.1335	**0.5284**
IM-27	0.3053	0.3002	0.1623	0.0689	**0.3621**
IM-28	0.5087	0.5052	0.4001	0.2537	**0.6944**
IM-29	0.3805	0.3778	0.4532	0.0630	**0.6964**
IM-30	0.4365	0.4305	0.3610	0.1080	**0.6407**

C. ENTROPY

The content of an information that is present in an image is measured through entropy function introduced by E. Shannon in 1948 [25] which is defined as follows:

$$H(I) = -\sum_{i=0}^{L} p_i \log p_i \tag{11}$$

In (11), I represent an image and p_i is the rate of recurrence of pixels with intensity i. Shannon's entropy states that, lesser the value of $H(I)$ designates information with low content, however on the other hand too high value of $H(I)$ indicates the presence of noise and double edges. Therefore, $H(I)$ should always lie in the middle of both extremes for best results. The graphical analysis of obtained results in comparison to previously proposed methods through entropy difference on human body parts are presented in Fig. 10.

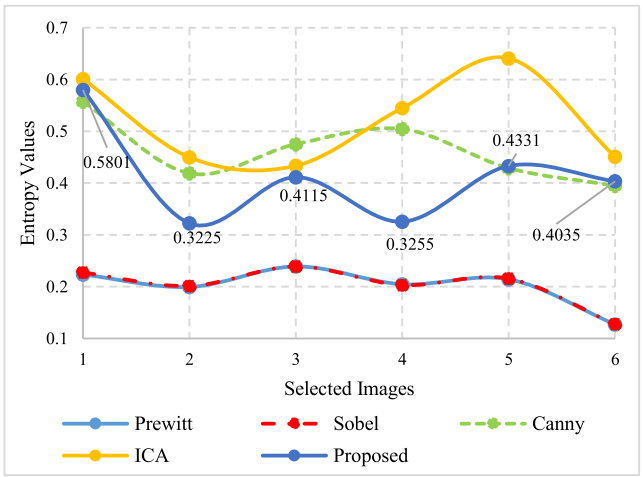

FIGURE 10. The graphical analysis of the results obtained from human body parts images in comparison of previously proposed methods through entropy.

The successful discovery of the meaningful edges is detected through the proposed approach. The attained entropy difference values are less than canny but higher than Prewitt's, Sobel's and relies nearby canny in some scenarios, which state that the entropy difference values fall in between the two extremes. Even though noise has been encountered in some cases, the acquired entropy difference values of the proposed approach are lesser than those of Canny and ICA. Therefore,

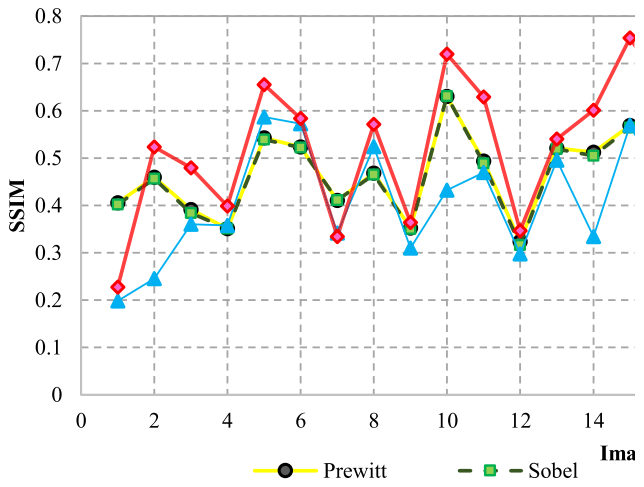

FIGURE 11. The graphical analysis of the obtained results in comparison of previously proposed methods through similarity.

it results in edges that restrain lesser noise proportions and more information content. Collectively, it also delivers the shade differences that is present in respective images. The obtained values of entropy difference for selected images are presented in Table III. Finally, it makes B-Edge algorithm a reliable method for MR images analysis of different body parts.

D. MSE (MEAN SQUARE ERROR) AND PSNR

The mean square error of the respective outcome is computed from (12).

$$MSE = \frac{1}{mn} \sum_{0}^{m-1} \sum_{0}^{n-1} ||O(s,t) - P(s,t)||^2 \quad (12)$$

Here, 'O' depicts the matrix data of source image, 'P' depicts the matrix data of obtained image, the total rows and columns count of the image pixels is presented as 'm' and 'n', 's' depicts the index value of rows and 't' depicts the index value of columns. The low MSE represents satisfactory edged results while a high MSE represents the non-acceptable outcomes [26].

The obtained values of MSE for images are presented in Table 4. It has been observed that the MSE values of Prewitt and Sobel are relatively higher for several images because of over segmentation as discussed earlier. Prewitt and Sobel's results overtake the results of Canny for image IM-1, IM-2, IM-26 and IM-27 in Table 4. In contrast, B-Edge achieves the minimum MSE values. A study reveals the lack of effectiveness in predicting the human response to image quality through PSNR method. Therefore, SSIM was introduced. PSNR has been computed from (13).

V. CONCLUSION

To overwhelm the issue of traditional approaches, our proposed method is capable to obtain desirable results from both normal and medical images. The proposed system encompasses a procedure that analyzes the further pieces of evidence from the image and connects the short contours into long ones. The obtained results are made compared with traditional algorithms. On observation, it is concluded that: 1) Developed method can successfully detect robust & thin edges with less noise proportion. 2) It provides with better edge continuity. 3) It provides better entropy value. There are several directions to improve B-Edge: 1) The proposal algorithm does not effectively work over blur images. 2) The time computation needs to be improved. 3) More optimal outcomes can be attained with the implementation with the deep learning approach. Finally, we would encourage that the future work to practice over more challenging databases. Better object detection and recognition can be acquired if the algorithm proposed is used in real time. This proposed edge detection method can be used in various device and application such as robots, automations, and medical equipment for safety, advancement and betterment of the society.

REFERENCES

[1] S. Loncaric, "A survey of shape analysis techniques," *Pattern Recognit.*, vol. 31, no. 8, pp. 983–1001, 1998.
[2] I. E. Abdou and W. K. Pratt, "Quantitative design and evaluation of enhancement/thresholding edge detectors," *Process. IEEE*, vol. 67, no. 5, pp. 753–763, May 1979.
[3] L. Kitchen and A. Rosenfeld, "Edge evaluation using local edge coherence," *IEEE Trans. Syst., Man, Cybern.*, vol. 11, no. 9, pp. 597–605, Sep. 1981.
[4] Q. Zhu, "Efficient evaluations of edge connectivity and width uniformity," *Image Vis. Comput.*, vol. 14, no. 1, pp. 21–34, 1996.
[5] O. Ghita and P. F. Whelan, "Computational approach for edge linking," *J. Electron. Imaging*, vol. 11, no. 4, p. 479, 2002.
[6] F. Russo, "Edge detection in noisy images using fuzzy reasoning," *IEEE Trans. Instrum. Meas.*, vol. 47, no. 5, pp. 1102–1105, Oct. 1998.
[7] W. Gao, X. Zhang, L. Yang, and H. Liu, "An improved Sobel edge detection," in *Proc. 3rd Int. Conf. Comput. Sci. Inf. Technol. (ICCSIT)*, Jul. 2010, pp. 67–71.
[8] S. Gupta and S. G. Mazumdar, "Sobel edge detection algorithm," *Int. J. Comput. Sci. Manag. Res.*, vol. 2, no. 2, pp. 1578–1583, 2013.
[9] S. E. El-Khamy, M. Lotfy, and N. El-Yamany, "A modified fuzzy Sobel edge detector," in *Proc. IEEE 17th Nat. Radio Sci. Conf.*, Feb. 2000, pp. 1–9.
[10] D.-S. Lu and C.-C. Chen, "Edge detection improvement by ant colony optimization," *Pattern Recognit. Lett.*, vol. 29, no. 4, pp. 416–425, 2008.
[11] P. Dollar, Z. Tu, and S. Belongie, "Supervised learning of edges and object boundaries," in *Proc. IEEE Comput. Soc. Conf. Comput. Vis. Pattern Recognit.*, Jun. 2006, pp. 1–8.
[12] P. Arbeláez, M. Maire, C. Fowlkes, and J. Malik, "Contour detection and hierarchical image segmentation," *IEEE Trans. Pattern Anal. Mach. Intell.*, vol. 33, no. 5, pp. 898–916, May 2011.
[13] J. J. Lim, C. L. Zitnick, and P. Dollár, "Sketch tokens: A learned mid-level representation for contour and object detection," in *Proc. IEEE Conf. Comput. Vis. Pattern Recognit.*, Jun. 2013, pp. 3158–3165.
[14] A. Agarwal and K. Goel, "Comparative analysis of digital image for edge detection by using bacterial foraging & canny edge detector," in *Proc. 2nd Int. Conf. Comput. Intell. Commun. Technol.*, Feb. 2016, pp. 125–129.
[15] Y. Yang, K. I. Kou, and C. Zou, "Edge detection methods based on modified differential phase congruency of monogenic signal," *Multidimensional Syst. Signal Process.*, vol. 29, no. 1, pp. 339–359, 2016.
[16] L. Xuan and Z. Hong, "An improved CANNY edge detection algorithm," in *Proc. 8th IEEE Int. Conf. Softw. Eng. Service Sci. (ICSESS)*, Nov. 2017, pp. 275–278.
[17] O. P. Verma and A. S. Parihar, "An optimal fuzzy system for edge detection in color images using bacterial foraging algorithm," *IEEE Trans. Fuzzy Syst.*, vol. 25, no. 1, pp. 114–127, Feb. 2017.

[18] M. A. Günen, Ü. H. Atasever, and E. Beşdok, "A novel edge detection approach based on backtracking search optimization algorithm (BSA) clustering," in *Proc. 8th Int. Conf. Inf. Technol. (ICIT)*, May 2017, pp. 116–122.
[19] X. Ma, S. Liu, S. Hu, P. Geng, M. Liu, and J. Zhao, "SAR image edge detection via sparse representation," *Soft Comput.*, vol. 22, no. 8, pp. 2507–2515, 2018.
[20] K. Zhang, Y. Zhang, P. Wang, Y. Tian, and J. Yang, "An improved Sobel edge algorithm and FPGA implementation," in *Proc. 8th Int. Congr. Inf. Commun. Technol.*, 2018, pp. 243–248.
[21] J. Cao, L. Chen, M. Wang, and Y. Tian, "Implementing a parallel image edge detection algorithm based on the Otsu-canny operator on the Hadoop platform," *Comput. Intell. Neurosci.*, vol. 2018, May 2018, Art. no. 3598284.
[22] R. Gonzalez and R. Woods, *Digital image processing*. 2002.
[23] J. Canny, "A computational approach to edge detection," *IEEE Trans. Pattern Anal. Mach. Intell.*, vol. PAMI-8, no. 6, pp. 679–698, Nov. 1986.
[24] W. Rong, Z. Li, W. Zhang, and L. Sun, "An improved CANNY edge detection algorithm," in *Proc. IEEE Int. Conf. Mechatron. Automat.*, 2014, vol. 2, no. 2, pp. 577–582.
[25] O. P. Verma, N. Agrawal, and S. Sharma, "An optimal edge detection using modified artificial bee colony algorithm," *Proc. Nat. Acad. Sci., India Sect. A, Phys. Sci.*, vol. 86, no. 2, pp. 157–168, 2016.
[26] P. Ganesan and V. Rajini, "Assessment of satellite image segmentation in RGB and HSV color space using image quality measures," in *Proc. Int. Conf. Adv. Elect. Eng.*, Jan. 2014, pp. 1–5.
[27] Z. Wang, A. C. Bovik, H. R. Sheikh, S. Member, E. P. Simoncelli, and S. Member, "Image quality assessment: From error visibility to structural similarity," *IEEE Trans. Image Process.*, vol. 13, no. 4, pp. 600–612, Apr. 2004.
[28] R. Laishram, W. K. Kumar, A. Gupta, and K. V. Prakash, "A novel MRI brain edge detection using PSOFCM segmentation and canny algorithm," in *Proc. Int. Conf. Electron. Syst., Signal Process. Comput. Technol. (ICESC)*, Jan. 2014, pp. 398–401.
[29] A. K. Ray, N. B. Bahadure, and S. Routray, "SVM-LWT enabled fuzzy clustering-based image analysis for brain tumor detection," *Int. J. Pure Appl. Math.*, vol. 117, no. 19, pp. 13–22, 2017.
[30] D. Bhawna, M. Neetu, and M. Megha, "Comparative analysis of edge detection techniques for medical images of different body parts," in *Proc. 4th Int. Conf. Recent Develop. Sci., Eng. Technol.*, 2017, pp. 164–176.
[31] Z. Unlu, Y. S. Tokmak, and A. Sahillioglu, "Suddenly developed hemorrhagic olecranon bursitis releated to traumatic asymptomatic heterotopic ossification," *Phys. Med. Rehabil. Res.*, vol. 2, no. 3, pp. 1–2, 2017.

MAMTA MITTAL received the degree in computer science and engineering from Kurukshetra University, Kurukshetra, in 2001, and the masters' degree (Hons.) in computer science and engineering from YMCA, Faridabad, and the Ph.D. degree in computer science and engineering from Thapar University Patiala. She was teaching from last 16 years with emphasis on data mining, machine learning, soft computing, and data structure. She is currently with the G.B. Pant Government Engineering College, New Delhi (under the Government of NCT Delhi), and also supervises Ph.D. candidates of Guru Gobind Singh Indraprastha University, Dwarka, New Delhi. She has published and communicated a number of research papers in SCI, SCIE, ESCI, and Scopus Indexed journals. She has attended many workshops, FDPs, and seminars. She is an active member of CSI.

AMIT VERMA from Kurukshetra University, Kurukshetra, India, and the Ph.D. degree in image processing. He is currently a young and innovative Academician and a Researcher. He is also the Head and a Professor with the Department of Computer Science Engineering, Chandigarh Engineering College. He has over 14 years of experience in teaching with two years of experience in industry. He has got the exposure of working with a telecommunication industry at Canada. He has guided around 60 students for their M.Tech. Thesis. He has been the Chair of various national and international conferences. He has always been actively involved in research and development. He has to his credit a number of research papers with a number of research publications in coveted and referred journals, including Springer and the IEEE. He is a Reviewer of various research journals. He is a Life Member of ISTE and ACM. His research interests include image processing, simulation and modeling, and face detection and recognition.

IQBALDEEP KAUR is currently an Associate Professor with the Department of Computer Science and Engineering, Chandigarh Engineering College, Mohali, India. Her research interests include machine learning, pattern recognition, classification, data mining, and knowledge discovery.

BHAVNEET KAUR received the B.Sc. degree (Hons.) in computer science from Delhi University and the M.C.A. degree from Sikkim Manipal University, in 2014. She is currently pursuing the Ph.D. degree in computer applications with the University Institute of Computing, Chandigarh University. Her research interests include digital image processing, computer vision, and computer graphics.

MEENAKSHI SHARMA received the M.C.A. degree (Hons.) and the M.Tech. and Ph.D. degrees in computer science and engineering from Kurukshetra University, in 2012. She is currently an Associate Professor and a Research Coordinator with the University Institute of Computing, Chandigarh University. Her research interests include data compression, digital image processing, and data warehousing.

LALIT MOHAN GOYAL received the B.Tech. (Hons.) in computer engineering from Kurukshetra University, Kurukshetra, the M.Tech. degree (Hons.) in information technology from Guru Gobind Singh Indraprastha University, New Delhi, and the Ph.D. degree in computer engineering from Jamia Millia Islamia, New Delhi. He has 16 years of teaching experience in the area of theory of computation, parallel and random algorithms, distributed data mining, and cloud computing. He is currently with the Department of Computer Engineering, J.C. Bose University of Science and Technology, YMCA, Faridabad, India. He is currently working on the project sponsored by the Indian Council of Medical Research, Delhi. He has published research papers in SCI indexed and Scopus indexed journals and conferences. He is a Reviewer of many reputed journals and conferences.

SUDIPTA ROY received the Ph.D. degree in computer science and engineering from the Department of Computer Science and Engineering, University of Calcutta. He is currently with the Radiological Chemistry and Imaging Laboratory, Washington University in Saint Louis, USA. He has more than five years of experience in teaching and research. He is an author of more than 30 publications in refereed national and international journals and conferences, including the IEEE, Springer, Elsevier, and many others. He is an author of one book and many book chapters. He holds an U.S. patent in medical image processing and filed an Indian patent in smart agricultural system. His research interests include biomedical image analysis, image processing, steganography, artificial intelligence, big data analysis, machine learning, and big data technologies. He is an International Advisory Committee Member and a Program Committee Member of many conferences. He has served as a Reviewer for many international journals, including the IEEE, Springer, Elsevier, IET, and many others, and international conferences. He is an Associate Editor of the IEEE ACCESS, IEEE journal, and an Editorial Member of the *International Journal of Computer Vision and Image Processing* and *IGI Global* Journal.

TAI-HOON KIM received the B.E. and M.E. degrees from Sungkyunkwan University, South Korea, and the Ph.D. degrees from the University of Bristol, U.K., and from the University of Tasmania, Australia. He is currently with the Department of Convergence Security, Sungshin Women's University, South Korea. He has published 300 research papers in international journals and conferences. His main research interests include security engineering for IT products, IT systems, development processes, and operational environments. He is an Editor of the Elsevier, Springer, and many more journals.